Atomic defects in the ordered compound $B2$-NiAl: A combination of *ab initio* electron theory and statistical mechanics

B. Meyer and M. Fähnle
Max-Planck-Institut für Metallforschung, Heisenbergstrasse 1, D-70569 Stuttgart, Germany
(Received 4 September 1998)

For an ideal model of a homogeneous thermodynamically stable ordered compound $B2$-Ni_xAl_{1-x} the effective formation energies and volumes of vacancies and antistructure atoms as well as the Ni and Al activities are calculated by a combination of the *ab initio* electron theory with a generalized grand canonical statistical approach. For nonstoichiometric compounds the structural defects are Ni vacancies (for $x<0.5$) or Ni antistructure atoms on the Al sublattice (for $x>0.5$). At stoichiometry ($x=0.5$) the calculated effective Ni vacancy formation energy agrees quite well with experimental data. For $x<0.5$ the theory predicts a shrinkage of the sample with increasing temperature (superimposed to the usual anharmonic lattice expansion) due to thermal annihilations of structural Ni vacancies, in contrast to the experimental observation. The reason for this discrepancy is probably deviations of the structure of real $B2$-Ni_xAl_{1-x} from the ideal model.
[S0163-1829(99)05609-X]

I. INTRODUCTION

$B2$-Ni_xAl_{1-x} is one of the promising candidates for high-temperature structural applications, and therefore numerous investigations of the mechanical properties were carried out in the past. Nevertheless, there is only little known about the formation and migration properties of atomic defects [vacancies and antistructure atoms on the two simple-cubic sublattices of the $B2$ (CsCl) structure] in these ordered compounds, which have a great influence on the mechanical creep resistance,[1] for instance. One of the problems for the investigation of the atomic defects is that it is very difficult to prepare samples with well-defined composition and good homogeneity which are in a thermodynamically stable state. Usually the uncertainties in the composition amount to 1 at. % at the stoichiometric composition ($x=0.5$), and it became possible only most recently[2] to reduce the uncertainty to 0.1 at. %. Because for Ni-poor systems structural vacancies appear (i.e., vacancies which survive even when going to zero temperature to guarantee the deviations from stoichiometry), even small deviations from stoichiometry have a strong influence on the defect structure. For nonstoichiometric samples local concentration inhomogeneities may appear within one single crystal due to seigering effects.[2] The formation of voids is observed[3,4] which may lead to an overestimation of the vacancy concentration when using density measurements. Finally, it is hard to prepare samples in thermodynamic equilibrium, on the one hand, because of the very slow annealing kinetics due to a high vacancy migration energy,[5] on the other hand, by vacancy supersaturation due to surface oxidation,[3,6] a suggestion made in Ref. 3 but questioned in Ref. 4.

In view of all the above discussed problems it appears that measurements on samples with nominally the same composition may yield drastically different results. For instance, the maximum plastic deformation obtained for six ''stoichiometric'' NiAl samples was 12.9% in one sample and 1–2.4 % in the five remaining samples.[7] Tracer diffusion measurements for the Ni atoms in well annealed NiAl samples[8] found a monotonic increase of the diffusion coefficient with increasing Ni content, in contrast to former measurements of Hancock and McDonnell[9] who found a minimum in the diffusion coefficient close to the stoichiometric composition and diffusion coefficients which were orders of magnitude larger. Finally, Zobel[10] obtained for $Ni_{47}Al_{53}$ an effective vacancy formation energy of 0.21 eV from differential thermal-expansion measurements, whereas time-differential thermal-expansion measurements[11] yielded a formation energy of (1.5 ± 0.25) eV for a sample with nominally the same composition. For a better understanding of the properties of $B2$-NiAl more experiments on well-defined samples[2,8,12,13] are indispensable.

In this complicated situation the help from theory is highly desirable, because there the ideal situation of a homogeneous thermodynamically stable compound can be considered. If the calculations are accurate enough, the quantitative results obtained for this model may serve as some kind of reference, and deviations between theory and experiment may be discussed in terms of possible deviations from this simple model occurring in real nature. The first calculations of this type were performed by the embedded-atom method,[14] and it was shown[15] that various forms of embedded-atom potentials fitted to various sets of input data may yield even qualitatively different results for the defect properties. An appropriate set of input data has to be chosen and the repulsive terms have to be adjusted accordingly in order to develop an embedded-atom potential which yields the correct structural defects for off-stoichiometric samples.[15,16] The *ab initio* calculations based on the local-density approximation[17] are free from all these ambiguities, however, they are very costly. The first *ab initio* calculations of the effective formation energies for stoichiometric $B2$-NiAl were performed by Fu *et al.*[18] within the framework of a supercell method with up to 32 atoms and the *ab initio* mixed-basis pseudopotential approach.[19] In the meanwhile, a more efficient and more accurate code for the

mixed-basis approach has been developed[20] which makes the use of larger supercells possible. The present paper reports on results for the effective formation energies for stoichiometric and nonstoichiometric NiAl obtained with this more accurate code for supercells containing up to 54 atoms. The results for the defect properties as functions of composition are compared with previous theoretical results and with experimental data. Finally, the effective defect formation volumes are calculated and discussed.

II. CALCULATIONAL METHOD

A. Statistical mechanics

The basic assumption of the theory is that the ordered compound A_xB_{1-x} is in a homogenous and thermodynamically stable state. As discussed in Sec. I this is hard to achieve in real nature, and therefore one way to interpret deviations between theoretical and experimental results is to relate them to deviations from this simple model occurring in nature. If we assume that the homogeneity of the ordered compound is conserved when raising the temperature then inevitably various types of atomic defects have to be generated simultaneously by thermal excitation.[21–25] Suppose, for instance, that only vacancies on the sublattice of the A atoms would be generated in thermal equilibrium. Then, with increasing temperature, more and more A atoms would be removed from the A-atom sublattice of the bulk and deposited at inner or outer surfaces, i.e., the homogeneity of the compound would be destroyed. The only way to avoid this problem is to generate simultaneously other types of atomic defects (i.e., vacancies on the other sublattice or antistructure atoms) with such a statistical weight that on the average the structure of the material is conserved.

To calculate the concentrations c_i^ν (i denotes the type of defect, i.e., vacancy or antistructure atom, and ν labels the sublattices α and β of the A and B atoms), a generalized grand canonical formalism was developed which in its most extended form is described in Refs. 21 and 22. This formalism is valid for small defect concentrations, i.e., at or close to stoichiometry and far from the order-disorder transition. The c_i^ν are obtained by minimizing an appropriate ansatz for the Gibbs free energy with respect to the numbers N_i^ν of various grand canonical defects (grand canonical vacancies which are obtained by totally removing an atom from the system, and grand canonical antistructure atoms where an atom on its own sublattice is replaced by an atom of the other type) which are introduced in the originally perfectly ordered compound. The conservation of particle numbers N_A and N_B is guaranteed by means of Lagrangian parameters μ_A and μ_B which have the meaning of chemical potentials. During the introduction of a grand canonical defect the energy, the volume, and the vibrational entropy of the system changes by ε_i^ν, ΔV_i^ν, and s_i^ν (defect formation parameters). We assume that for small defect concentrations these defect formation parameters are independent of the defect concentrations. The minimization of the Gibbs free energy yields the concentrations $c_i^\nu = N_i^\nu/2M$ ($2M$ is the total number of lattice sites) as function of temperature T, pressure p, and chemical potentials μ_A and μ_B. For instance, for the concentration of vacancies on the α sublattice or A antistructure atoms on the β sublattice we find

$$c_v^\alpha = \frac{1}{2}\,\frac{e^{s_v^\alpha/k_B} e^{-(\varepsilon_v^\alpha+\mu_A+p\Delta V_v^\alpha)/k_BT}}{1+e^{s_v^\alpha/k_B} e^{-(\varepsilon_v^\alpha+\mu_A+p\Delta V_v^\alpha)/k_BT}+e^{s_B^\alpha/k_B} e^{-(\varepsilon_B^\alpha+\mu_A-\mu_B+p\Delta V_B^\alpha)/k_BT}}, \tag{1}$$

$$c_A^\beta = \frac{1}{2}\,\frac{e^{s_A^\beta/k_B} e^{-(\varepsilon_A^\beta-\mu_A+\mu_B+p\Delta V_A^\beta)/k_BT}}{1+e^{s_A^\beta/k_B} e^{-(\varepsilon_A^\beta-\mu_A+\mu_B+p\Delta V_A^\beta)/k_BT}+e^{s_v^\beta/k_B} e^{-(\varepsilon_v^\beta+\mu_B+p\Delta V_v^\beta)/k_BT}}. \tag{2}$$

The chemical potentials $\mu_A(T,p,x)$ and $\mu_B(T,p,x)$ are derived from the Gibbs-Duhem relation, which yields

$$\varepsilon_0 + p\Omega_0 - Ts_0 = \mu_A + \mu_B - k_BT \ln[(1-2c_v^\alpha-2c_B^\alpha)(1-2c_v^\beta-2c_A^\beta)], \tag{3}$$

where ε_0, Ω_0, and s_0 denote the energy, volume, and vibrational entropy of the ideal elementary unit cell $A_{0.5}B_{0.5}$, and from the equation

$$\frac{N_A}{N_B} = \frac{x}{1-x} = \frac{1-2c_v^\alpha-2c_B^\alpha+2c_A^\beta}{1-2c_v^\beta-2c_A^\beta+2c_B^\alpha}, \tag{4}$$

which guarantees the correct composition of the compound. In general these two equations have to be solved numerically, and then the concentrations c_i^ν may be calculated from Eqs. (1) and (2) as complicated functions of T, p, and x. However, if the temperature and pressure dependences of the chemical potentials may be linearized in the experimental ranges, Eqs. (1) and (2) may be approximated[23] by simple exponentials

$$c_i^\nu = \frac{1}{2} e^{\tilde{S}_i^\nu/k_B} e^{-(\tilde{E}_i^\nu + p\tilde{\Omega}_i^\nu)/k_BT}. \tag{5}$$

The effective formation entropy $\tilde{S}_i^\nu$, energy $\tilde{E}_i^\nu$, and volume $\tilde{\Omega}_i^\nu$ then may be obtained from the concentrations $c_i^\nu(T,p,x)$ as in a monoatomic crystal, i.e., $\tilde{S}_i^\nu$ is found by extrapolating $\ln c_i^\nu(1/T)$ to $1/T \to 0$, and

$$\tilde{E}_i^\nu = -k_B \frac{\partial \ln c_i^\nu}{\partial(1/T)}, \tag{6}$$

$$\tilde{\Omega}_i^\nu = -k_B T \frac{\partial \ln c_i^\nu}{\partial p}. \quad (7)$$

However, because in ordered compounds inevitably various types of defects have to be generated simultaneously, the physical interpretation of these effective formation quantities is much more complicated than in monoatomic crystals (see Refs. 21–25 and Appendix A). If certain preconditions are fulfilled, approximate analytical expressions for the linear temperature and pressure dependences of μ_A and μ_B and hence analytical expressions for the effective formation quantities may be obtained from Eqs. (1)–(4). For nonstoichiometric compounds this is the case if the concentrations of thermal defects is much smaller than the concentration of the structural defect and if the type of structural defect is known (e.g., from preceding numerical calculations). For stoichiometric compounds this is the case if the defect concentrations are small and two types of defects (those with the smallest effective formation energies) dominate strongly. If these preconditions are fulfilled then it is possible to select from the many possible defect combinations which conserve the homogeneity of the sample and which involve a specific defect under consideration a special defect combination by which the considered defect is generated most effectively. Then the analytical expressions for the effective defect formation quantities derived in Appendix A tell us what this special defect combination looks like. If the above discussed preconditions are not fulfilled, for instance, if more than two defects coexist with comparable concentrations in some temperature range [as is probably the case in $B2$-FeAl (Refs. 22–24)], then several or even many different defect combinations may contribute to the generation of the considered defect, and then the concentrations have to be determined numerically from Eqs. (1)–(4).

Please note that because of our approximation of defect formation parameters which do not depend on the concentration of the defects and as a consequence of the approximations involved in the analytical calculation the analytical expressions for the effective formation energies exhibit a discontinuous behavior: They are independent of the composition for $x<0.5$ and $x>0.5$, but they attain different values for $x<0.5$, $x=0.5$, and $x>0.5$. In contrast, the analytic expressions for the effective formation entropies change with composition in the whole composition range (see Appendix A). They diverge for $x\rightarrow 0.5$, however, it must be taken into account that our approximation adopted for the derivation of the analytical expressions (i.e., the concentration of structural defects is much larger than the concentration of thermal defects) holds for progressively smaller temperatures T when approaching the stoichiometric composition more and more.[25] In order to obtain the concentrations close to stoichiometry at finite temperatures, one has to solve Eqs. (1)–(4) numerically, and this of course yields concentrations which vary smoothly with T and x.[18,23,26]

The structural defect, i.e., the one which survives when going to zero temperature may be identified from the concentration equations as the one for which $\tilde{E}_i^\nu + p\tilde{\Omega}_i^\nu = 0$, i.e., $\tilde{E}_i^\nu = 0$ for zero p. According to Appendix A, in addition to the structural defects which appear even at zero temperature, defects of the same type may be generated or annihilated together with the thermal excitations of the nonstructural defects.

B. *Ab initio* electron theory

In the following we calculate the defect formation parameters ε_i^ν and ΔV_i^ν by the *ab initio* electron theory. The defect entropy parameters s_i^ν are neglected because it is extremely costly to calculate them *ab initio*.[27] This has only a very small influence on the effective formation energies and volumes,[25] but of course we cannot discuss the absolute values of the concentrations when using this approximation.

The defect formation parameters ε_i^ν and ΔV_i^ν were calculated by a supercell approach, i.e., large supercells containing N sites and one defect, respectively, were arranged periodically and ε_i^ν or ΔV_i^ν was determined from the difference in energy or equilibrium volume of the supercells with and without the defect. Supercells containing $N=16$ and 54 atoms were considered. The calculations were performed by the *ab initio* electron theory in local-density approximation[17,28] and the *ab initio* pseudopotential method[29] (including the partial core correction[30]) with a mixed-basis set[19,20] consisting of plane waves and five localized and nonoverlapping d orbitals per Ni atom. For this mixed-basis pseudopotential method a highly efficient code has been developed recently[20] in which in addition former approximations for the matrix elements of the local part of the pseudopotential involving localized orbitals were removed, which improved the accuracy of the total energy and force calculation. The structural relaxations of the atoms surrounding the defects were fully taken into account. For the sampling of the Brillouin zone the special k points of Chadi and Cohen[31] and Gaussian broadening[32,33] with a smearing parameter of 0.1 eV were used. For the calculation of the cohesive properties of the ideal stoichiometric compound $B2$-NiAl the results were converged with respect to the plane-wave cutoff E_{pw} and the number of k points. For the supercell calculations the energies still can be reasonably converged with respect to the number of k points, but the energies are usually quite far from being converged with respect to E_{pw}. It is shown in Appendix B that — nevertheless — well converged results for the effective formation energies and volumes may be obtained from supercell calculations which are not yet converged with respect to E_{pw}.

III. RESULTS

Concerning the cohesive properties of ideal stoichiometric $B2$-NiAl, we determined a lattice parameter of $a_0 = 2.837$ Å, a bulk modulus of $B_0 = 185$ GPa, and a cohesive energy per unit cell of $E_{\mathrm{coh}} = -11.5$ eV, compared to the experimental results at room temperature of $a_0 = 2.886$ Å (Ref. 34) and $B_0 = 158$ GPa.[35] We thus obtained a slight overbinding, as is usual for the local density approximation.

Table I exhibits for unrelaxed supercells with the lattice constant $a_0 = 2.84$ Å some tests for the convergence of the effective formation energies of the stoichiometric system with respect to the supercell size, the plane-wave cutoff E_{pw}, and the number n_k of equivalent k points in the irreducible

TABLE I. Convergence tests with respect to the supercell size N, the number n_k of equivalent k points in the irreducible part of the Brillouin zone of the ideal two atom unit cell, and the plane-wave cutoff $E_{\rm pw}$ (in Ry). The calculations were performed for unrelaxed supercells of stoichiometric NiAl at the equilibrium lattice constant $a_0=2.84$ Å of the ideal unit cell, and the effective formation energies (in eV) are given for the stoichiometric composition. The effective formation energies $\tilde{E}_v^\alpha$ and $\tilde{E}_{\rm Ni}^\beta$ are identical because stoichiometric NiAl is a triple defect system (see Sec. IV).

N	n_k	$E_{\rm pw}$	$\tilde{E}_v^\alpha$	$\tilde{E}_v^\beta$	$\tilde{E}_{\rm Ni}^\beta$	$\tilde{E}_{\rm Al}^\alpha$
16	20	12.5	0.97	2.12	0.97	2.83
	56	12.5	1.00	2.13	1.00	2.86
		16.0	0.99	2.13	0.99	2.84
	120	12.5	0.97	2.09	0.97	2.77
54	20	12.5	0.77	1.99	0.77	2.65
	56	12.5	0.88	2.09	0.88	3.00
		16.0	0.88	2.08	0.88	2.99
	120	12.5	0.83	2.01	0.83	2.83

part of the Brillouin zone of the ideal two atom unit cell. There are only slight differences between the results for the two supercell sizes. These differences become larger (Table II) when allowing for the structural relaxation of the atoms around the defects and a subsequent volume relaxation of the supercell (while fixing the scaled positions of the atoms). Therefore, the final results for the effective formation energies were obtained for the 54 atom supercell. The structural relaxation has a stronger effect than the volume relaxation. It is of the order of magnitude of a few percent or of a few tenths of a percent of the equilibrium lattice constant, being strongest for the Al antistructure atom on the α sublattice (Table III). For the Al vacancy all surrounding atoms relax towards the vacancy, whereas for all the other defects there is an oscillatory relaxation behavior of the surrounding atoms. The volume relaxation yields defect volume parameters ΔV_i^ν of $-28,-47,-26$, and $+55\%$ of the average volume per atom $\Omega_0/2$ of the ideal two atom unit cell for the α vacancy, the β vacancy, the Ni antistructure atom on the β sublattice and the Al antistructure atom on the α sublattice, respectively. It becomes obvious from Table I that the convergence of the results with respect to the number n_k of k points is not critical, and for the final calculations including the relaxations we used $n_k=56$. Finally, the results are already very well converged for $E_{\rm pw}=12.5$ Ryd because the numerical procedure described in Appendix B is adopted. The final results for the effective formation energies and volumes obtained from the analytical expressions derived in Appendix A for various compositions are given in Table IV.

Figure 1 represents the Al activities

$$\ln\frac{a_{\rm Al}(x)}{a_{\rm Al}(x=0.5)}=[\mu_{\rm Al}(x)-\mu_{\rm Al}(x=0.5)]/k_BT \qquad (8)$$

as function of the composition for $T=1273$ K, which may be obtained experimentally by an isopiestic method,[36] for instance. The solid curve shows the results which are obtained numerically from Eqs. (1)–(4) when considering zero pressure p, zero defect entropy parameters s_i^ν and zero s_0.

TABLE II. The effect of structural relaxation and volume relaxation on the effective formation energies (in eV) of stoichiometric NiAl. The calculations were performed for $E_{\rm pw}=12.5$ Ry and $n_k=56$. The effective formation energies $\tilde{E}_v^\alpha$ and $\tilde{E}_{\rm Ni}^\beta$ are identical because stoichiometric NiAl is a triple defect system (see Sec. IV).

N	Relaxation	$\tilde{E}_v^\alpha$	$\tilde{E}_v^\beta$	$\tilde{E}_{\rm Ni}^\beta$	$\tilde{E}_{\rm Al}^\alpha$
16	Without	1.00	2.13	1.00	2.86
	Structural	0.97	2.11	0.97	2.49
	Struct.+vol.	0.95	2.03	0.95	2.37
54	Without	0.88	2.09	0.88	3.00
	Structural	0.76	2.01	0.76	2.40
	Struct.+vol.	0.74	1.97	0.74	2.36

The activities were also calculated from the analytical approximations for the chemical potentials (Appendix A), yielding

$$\ln\frac{a_{\rm Al}(x)}{a_{\rm Al}(x=0.5)}=\begin{cases}\frac{1}{3}G_0/k_BT-\frac{1}{3}\ln 2+\ln\frac{1-2x}{1-x} & \text{for } x<0.5\\ -\frac{1}{6}G_0/k_BT-\frac{1}{3}\ln 2+\frac{1}{2}\ln\frac{4(1-x)^2}{2x-1} & \text{for } x>0.5\end{cases} \qquad (9)$$

with

$$G_0=2\tilde{E}_v^\alpha+\tilde{E}_{\rm Ni}^\beta+p(2\tilde{\Omega}_v^\alpha+\tilde{\Omega}_{\rm Ni}^\beta)-T[2\tilde{S}_v^\alpha(x=0.5)+\tilde{S}_{\rm Ni}^\beta(x=0.5)], \qquad (10)$$

where the constant G_0 does not depend on the concentration x. It turned out that the results of the numerical and the analytical calculations agreed more or less perfectly except for a range of compositions very close to the stoichiometric one. This gives us the possibility to fit Eq. (9) outside this range to the experimental data reported in Ref. 37, whereby for $p=0$ the only fit parameter is the sum of the effective formation entropies $2\tilde{S}_v^\alpha(x=0.5)+\tilde{S}_{\rm Ni}^\beta(x=0.5)$. The dotted curve of Fig. 1 shows that a very good fit is obtained for $2\tilde{S}_v^\alpha(x=0.5)+\tilde{S}_{\rm Ni}^\beta(x=0.5)=2.25\ k_B$. The dashed curve in Fig. 1 shows the numerical results for the Ni activities (for $p=0$ and $s_i^\nu=s_0=0$) for which so far no experimental data are available.

IV. DISCUSSION

In this paper we considered the properties of atomic defects for an ideal homogeneous thermodynamically stable $B2$ phase of NiAl. The concentrations of the various defects were obtained by a generalized grand canonical approach. The only additional approximation entering this approach is the assumption that the defect formation parameters are independent of the defect concentrations, which restricts the applicability of the method to compositions close to stoichiometry and to temperatures far below the order-disorder tran-

TABLE III. Relaxations of the atoms surrounding a defect in various neighbor shells (in atomic units a.u.). The numbers in parentheses are the relative displacements in percent of the equilibrium lattice constant of ideal stoichiometric NiAl. A negative sign means that the atom moves towards the defect. The calculations were performed at the equilibrium lattice constant and for $E_{\mathrm{pw}}=12.5$ Ry, $n_k=56$.

Shell	N	Ni-v	Al-v	Ni-as	Al-as
1	16	−0.059 (1.1%)	−0.018 (0.3%)	−0.004 (0.1%)	+0.144 (2.7%)
	54	−0.110 (2.0%)	−0.026 (0.5%)	+0.029 (0.5%)	+0.223 (4.2%)
2	16				
	54	+0.084 (1.6%)	−0.069 (1.3%)	−0.110 (2.0%)	−0.134 (2.5%)
3	16				
	54	−0.031 (0.6%)	−0.017 (0.3%)	+0.006 (0.1%)	+0.028 (0.5%)

sition. Various types of canonical approaches have been developed[15,38] in the past which yield identical results so that there are no doubts on the validity of the statistical method. The defect formation parameters appearing in the statistical approach were calculated by the *ab initio* electron theory in the local-density approximation. This calculation method yields results for the vacancy formation energies of elementary Li, Na, K, Al, and Mo in excellent agreement with experimental data.[39] Because there is no reason why the method should fail for the intermetallic compounds, we assume that our *ab initio* method is indeed highly reliable and accurate. Altogether, it becomes clear that strong differences between theory and experiment for the effective formation energies mean that real NiAl considered in the experiments may not be described by the ideal model of a homogeneous thermodynamically stable $B2$ phase (inhomogeneities which act as sinks or sources of atoms, different phases, deviations from thermodynamical stability due to inhomogeneities or to a very slow annealing kinetics, etc.). Slight deviations may be related to the assumption of concentration independent defect formation parameters, to a weak deficiency of the local-density approximation or to not perfectly converged *ab initio* calculations (see Sec. III).

For a comparison with experiments it should be recalled that the vibrational entropy parameters were neglected so that we cannot expect quantitative results for the absolute concentrations c_i^{ν}. We therefore restrict our discussion to the effective formation energies.

According to Table IV, stoichiometric NiAl is a triple-defect system, i.e., two Ni vacancies on the α sublattice and one Ni antistructure atom on the Al sublattice are generated simultaneously. The effective formation energy for Ni vacancies and Ni antistructure atoms is 0.74 eV, whereas the effective formation energies for the Al vacancy on the β sublattice and the Al antistructure atom are much larger so that the precondition for the application of the analytical expressions of Appendix A is certainly fulfilled. Our effective formation energy for the Ni vacancy is slightly smaller than the one obtained by Fu *et al.*[18] (0.93 eV), which was obtained with the former less accurate mixed-basis code and for a supercell with 32 rather than 54 atoms. It is slightly larger than the value of 0.68 eV obtained by Mishin and Farkas[16] with the embedded-atom method and the value of 0.65 eV

TABLE IV. Effective formation energies (in eV) and volumes (in units of the average volume per atom $\Omega_0/2$ of the ideal two atom unit cell) for NiAl at various compositions.

	$x>0.5$	$x=0.5$	$x<0.5$
$\tilde{E}_v^{\alpha}$	1.11	0.74	0.0
$\tilde{E}_v^{\beta}$	1.60	1.97	2.71
$\tilde{E}_{\mathrm{Ni}}^{\beta}$	0.0	0.74	2.22
$\tilde{E}_{\mathrm{Al}}^{\alpha}$	3.10	2.36	0.88
$\tilde{\Omega}_v^{\alpha}$	0.59	0.40	0.0
$\tilde{\Omega}_v^{\beta}$	0.66	0.86	1.26
$\tilde{\Omega}_{\mathrm{Ni}}^{\beta}$	0.0	0.40	1.19
$\tilde{\Omega}_{\mathrm{Al}}^{\alpha}$	0.29	−0.11	−0.90

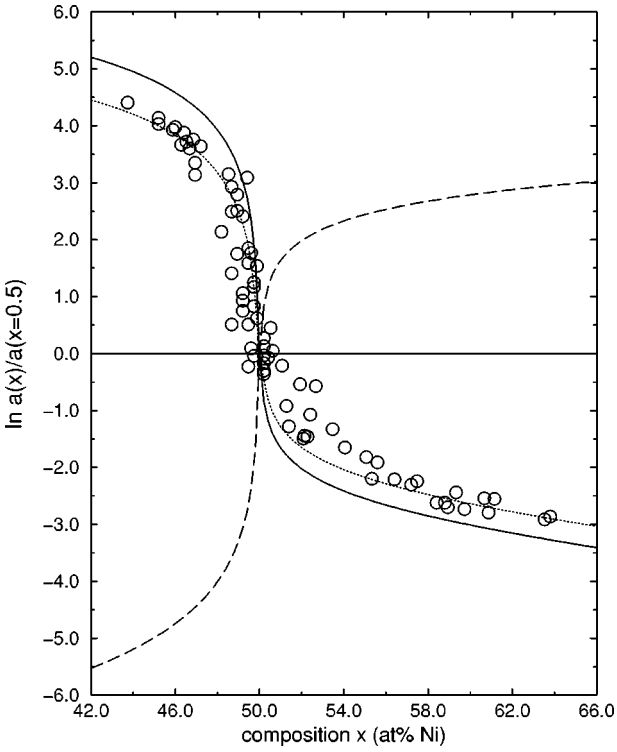

FIG. 1. Activities of Al in NiAl at $T=1273$ K as a function of the composition x. The solid curve is calculated with zero defect entropy parameters. The dotted curve is the result after fitting the entropy terms (see text). The experimental data points are taken from Krachler *et al.* (Ref. 37). The dashed curve represents our numerical results for the activity of the Ni atom as calculated by neglecting the entropy terms.

found by Badura-Gergen[40] with the empirical Bragg-Williams method. For the Al vacancy, however, the embedded-atom method of Mishin and Farkas yields a value of 1.23 eV which is much smaller than our *ab initio* value of 1.97 eV. The only experimental value of 0.68 eV for the effective Ni vacancy formation energy of stoichiometric NiAl from differential thermal-expansion measurements[10] agrees quite well with the theoretical data.

In the case of nonstoichiometric systems we obtain as structural defects Ni vacancies on the α sublattice for $x<0.5$ and Ni antistructure atoms on the β sublattice for $x>0.5$. Structural Ni vacancies were also found in $D0_3$-Ni_3Sb by coherent elastic neutron-scattering experiments[41] and by the *ab initio* electron theory.[26] Thus the early suggestion of Bradley and Taylor,[42] who explained their combined measurements of the density and the lattice parameter for various compositions in terms of these structural defects, is confirmed. For $x>0.5$ the effective formation energies are smallest for the vacancies on the two sublattices, i.e., in this case the self-diffusion may be mediated by vacancies on both sublattices, whereas in the model system of a homogeneous thermodynamically stable $B2$-FeAl there is only a very small concentration of Al vacancies for all compositions.[22,23,39] For $x<0.5$ the effective formation energy is by far smallest for the Al antistructure atom on the α sublattice (0.88 eV), whereby two Ni vacancies are annihilated during the thermal creation of an Al antistructure atom (see Appendix A). As a result, we expect a shrinkage of the Ni-poor samples with increasing temperature, superimposed to the usual anharmonic lattice expansion, with an activation energy of 0.88 eV. The effective formation energy of the Al vacancy on the β sublattice is rather high for $x<0.5$ which might explain the most recent observation[8] that the Ni diffusion constant is smaller for $x<0.5$ than for $x>0.5$, although there are structural Ni vacancies in abundance for $x<0.5$.

The only experimental data for the effective vacancy formation energies of Ni-poor NiAl are from differential thermal-expansion measurements[10] and from time-differential thermal-expansion measurements.[11] In both experiments it seems to be clear that there is an expansion rather than a shrinkage of the sample with increasing temperature. Quantitatively, however, there are considerable differences: Both techniques consider a sample of nominally the same composition ($Ni_{47}Al_{53}$), but the differential thermal expansion[10] yields an effective formation energy of 0.21 eV, whereas the time-differential thermal expansion gives (1.5 $\pm$0.25) eV. In our opinion both the qualitative difference between theory and experiment as well as the considerable quantitative difference between the two experiments is a strong hint that possibly the samples cannot be described by the ideal model of a homogeneous thermodynamically stable $B2$ phase. It should be noted that, in principle, there is a second possibility to explain the qualitative difference between theory and experiment. So far we have assumed that for $x<0.5$ the dominant thermal defects are Al antistructure atoms on the α sublattice because their effective formation energy of 0.88 eV is much smaller than those for the Ni antistructure atom on the β sublattice (2.22 eV) or the Al vacancy on the β sublattice (2.71 eV). In principle, it could be (although this is not very likely) that the vibrational defect entropy parameters (which we neglected in our calculations) favor the Ni antistructure atoms on the β sublattice so strongly that their concentration exceeds the concentration of the Al antistructure atom on the α sublattice in spite of the considerably larger effective formation energy. Because in that case two Ni vacancies on the α sublattice have to be generated simultaneously with the Ni antistructure atom, the crystal would expand with increasing temperature, however, with an activation energy of 2.22 eV which is much larger than the two experimental values (0.21 and 1.5 eV). Finally, it might also be that our assumption of defect formation parameters which are independent of the defect concentrations fails which, however, is also unlikely because the deviation from stoichiometry was small for the considered sample and the thermal defect concentration at the investigated temperatures [$T<1000$ K (Ref. 11)] was also small because of the high order-disorder transition temperature of NiAl. Altogether, we think that the first explanation is most likely.

Kim *et al.*[6] have investigated the concentration of atomic defects for various compositions and two temperatures (1173 and 1573 K) by the neutron-diffraction technique. This very difficult experiment yielded hints to the existence of Al vacancies and Al antistructure atoms in considerable concentrations (about 1%) in addition to the Ni vacancies and Ni antistructure atoms. Because we did not calculate the absolute defect concentrations, we cannot comment on these results.

The defect volume parameter ΔV_i^ν is largest and positive for the Al antistructure atom on the α sublattice, indicating a large effective size of the Al atom. Nevertheless, the effective formation volume of the Al antistructure atom is strongly negative for $x<0.5$, weakly negative for $x=0.5$, and slightly positive for $x>0.5$. The reason is that the effective formation volume as obtained from Eq. (7) is not only determined by the defect volume parameter of the considered defect, but by a combination of the defect volume parameters of all defects which have to be generated simultaneously with the considered defect in order to conserve the homogeneity of the material. According to Eq. (A16) we have for $x>0.5$ and for the case that Ni antistructure atoms on the β sublattice are the structural defects the relation

$$\tilde{\Omega}_{\mathrm{Al}}^{\alpha}=\Delta V_{\mathrm{Al}}^{\alpha}+\Delta V_{\mathrm{Ni}}^{\beta}, \tag{11}$$

which yields a positive value because of $|\Delta V_{\mathrm{Al}}^{\alpha}|>|\Delta V_{\mathrm{Ni}}^{\beta}|$, $\operatorname{sign}\Delta V_{\mathrm{Al}}^{\alpha}=-\operatorname{sign}\Delta V_{\mathrm{Ni}}^{\beta}=+1$. The underlying physical mechanism is that A and B atoms exchange sites between the α and β sublattice. For $x=0.5$ and a triple defect system we have Eq. (A11)

$$\tilde{\Omega}_{\mathrm{Al}}^{\alpha}=\Delta V_{\mathrm{Al}}^{\alpha}-\frac{1}{3}(\Omega_0+2\Delta V_v^{\alpha}-2\Delta V_{\mathrm{Ni}}^{\beta}), \tag{12}$$

which yields a slightly negative value (Ω_0 is the equilibrium volume of the two atom unit cell). Equation (12) tells us that Al antistructure atoms on the Ni sublattice are most effectively generated on the statistical average by producing three Al antisite atoms while simultaneously removing an elementary unit cell from the surface, annihilating two α vacancies and creating two Ni antistructure atoms on the β sublattice. Finally, for $x<0.5$ and structural α vacancies we obtain Eq. (A19)

$$\tilde{\Omega}^{\alpha}_{\mathrm{Al}} = \Delta V^{\alpha}_{\mathrm{Al}} - \Omega_0 - 2\Delta V^{\alpha}_{v}, \tag{13}$$

which yields a strongly negative value. The mechanism now is that an Al and a Ni atom are removed from the surface. The Ni atom is inserted into one α vacancy which is annihilated and the Al atom is inserted into another α vacancy, creating the Al antistructure atom. It becomes apparent from this discussion that the effective formation volumes have to be discussed very carefully in order to avoid serious misinterpretations of experimental data.[21,22,24,39]

V. CONCLUSION

It is well known that the experimental investigation of atomic defects in $B2$-NiAl is highly critical because it is a problem to produce well-defined samples. In the present paper, therefore, some kind of reference is given by calculating the defect structure for an ideal model of a homogeneous thermodynamically stable ordered compound. Differences between theory and experiment then may be traced back to deviations from this simple model occurring in real nature. The calculations yield the correct structural defects, and at stoichiometry the calculated effective vacancy formation energy agrees well with available experimental data. Discrepancies among various experiments and even qualitative differences between theory and experiment appear for Ni-poor system: In contrast to the experiments the theory predicts a shrinkage of the sample due to a thermally activated annihilation of structural Ni vacancies with increasing temperature (superposed to the usual anharmonic lattice expansion). It is concluded that all these problems probably arise from deviations of the structure of the real samples from the ideal model considered in the theory.

ACKNOWLEDGMENTS

The authors are indebted to G. Bester and H.-E. Schaefer for helpful discussions.

APPENDIX A

As discussed in Sec. II A, analytical expressions for the effective defect formation quantities may be obtained if certain preconditions are fulfilled. We illustrate the prescription how these effective formation quantities are obtained for one example in the stoichiometric and for one in the nonstoichiometric case and give a list of these quantities for all other conceivable cases.

1. The stoichiometric case

In the stoichiometric case, Eq. (4) reduces to

$$c^{\alpha}_{v} + 2c^{\alpha}_{B} = c^{\beta}_{v} + 2c^{\beta}_{A}, \tag{A1}$$

and for small defect concentrations Eq. (3) may be approximated by

$$\varepsilon_0 + p\Omega_0 - Ts_0 = \mu_A + \mu_B. \tag{A2}$$

Analytical expressions may now be obtained if two types of defects dominate strongly. This entails that the effective defect formation quantities are identical for those two types of defects, as can be seen in the following example:

(1) Vacancy-type systems.

If the vacancies on the two sublattices have the smallest effective formation energies and dominate strongly, then Eq. (A1) reduces further to

$$c^{\alpha}_{v} = c^{\beta}_{v}, \tag{A3}$$

where we can use the expression (1) for the concentrations, thereby neglecting for small defect concentrations the exponentials in the denominators. Equations (A2) and (A3) then yield the chemical potentials, and by inserting these quantities into Eqs. (1) and (2) and neglecting again the exponentials in the denominators, the concentrations c^{ν}_{i} may be written in the form of Eq. (5) with the following effective defect formation quantities:

$$\begin{aligned}
\tilde{E}^{\alpha}_{v} &= \tilde{E}^{\beta}_{v} = \tfrac{1}{2}(\varepsilon_0 + \varepsilon^{\alpha}_{v} + \varepsilon^{\beta}_{v}),\\
\tilde{E}^{\beta}_{A} &= \varepsilon^{\beta}_{A} + \varepsilon^{\alpha}_{v} - \varepsilon^{\beta}_{v},\\
\tilde{E}^{\alpha}_{B} &= \varepsilon^{\alpha}_{B} - \varepsilon^{\alpha}_{v} + \varepsilon^{\beta}_{v},
\end{aligned} \tag{A4}$$

$$\begin{aligned}
\tilde{\Omega}^{\alpha}_{v} &= \tilde{\Omega}^{\beta}_{v} = \tfrac{1}{2}(\Omega_0 + \Delta V^{\alpha}_{v} + \Delta V^{\beta}_{v}),\\
\tilde{\Omega}^{\beta}_{A} &= \Delta V^{\beta}_{A} + \Delta V^{\alpha}_{v} - \Delta V^{\beta}_{v},\\
\tilde{\Omega}^{\alpha}_{B} &= \Delta V^{\alpha}_{B} - \Delta V^{\alpha}_{v} + \Delta V^{\beta}_{v},
\end{aligned} \tag{A5}$$

$$\begin{aligned}
\tilde{S}^{\alpha}_{v} &= \tilde{S}^{\beta}_{v} = \tfrac{1}{2}(s_0 + s^{\alpha}_{v} + s^{\beta}_{v}),\\
\tilde{S}^{\beta}_{A} &= s^{\beta}_{A} + s^{\alpha}_{v} - s^{\beta}_{v},\\
\tilde{S}^{\alpha}_{B} &= s^{\alpha}_{B} - s^{\alpha}_{v} + s^{\beta}_{v}.
\end{aligned} \tag{A6}$$

All these equations have simple physical interpretations. The equations for the two vacancies reflect the fact that both vacancies have to be generated simultaneously, thereby enlarging the crystal by one elementary unit cell. The equation for the A antistructure atom on the β sublattice tells us that it is generated by transferring an A atom from the α sublattice to a vacancy on the β sublattice, etc. Please note that the effective formation quantities of a defect (i,ν) do not depend just on the defect formation parameters $\varepsilon^{\nu}_{i}, s^{\nu}_{i}, \Delta V^{\nu}_{i}$ of the same defect, but they contain also the defect formation parameters from the defects which have to be generated or annihilated simultaneously. This holds also for all the other cases discussed in this appendix, and this must be taken into account to avoid misinterpretations of experimental data.[21–25,39]

(2) Antistructure-type systems.

$$\begin{aligned}
\tilde{E}^{\alpha}_{v} &= \varepsilon^{\alpha}_{v} + \tfrac{1}{2}\left(\varepsilon_0 + \frac{\varepsilon^{\beta}_{A} - \varepsilon^{\alpha}_{B}}{2}\right),\\
\tilde{E}^{\beta}_{v} &= \varepsilon^{\beta}_{v} + \tfrac{1}{2}\left(\varepsilon_0 - \frac{\varepsilon^{\beta}_{A} - \varepsilon^{\alpha}_{B}}{2}\right),\\
\tilde{E}^{\alpha}_{B} &= \tilde{E}^{\beta}_{A} = \tfrac{1}{2}(\varepsilon^{\beta}_{A} + \varepsilon^{\alpha}_{B}),
\end{aligned} \tag{A7}$$

$$\tilde{\Omega}^{\alpha}_{v} = \Delta V^{\alpha}_{v} + \tfrac{1}{2}\left(\Omega_0 + \frac{\Delta V^{\beta}_{A} - \Delta V^{\alpha}_{B}}{2}\right),$$

$$\tilde{\Omega}_v^\beta = \Delta V_v^\beta + \tfrac{1}{2}\left(\Omega_0 - \frac{\Delta V_A^\beta - \Delta V_B^\alpha}{2}\right),$$

$$\tilde{\Omega}_B^\alpha = \tilde{\Omega}_A^\beta = \tfrac{1}{2}(\Delta V_A^\beta + \Delta V_B^\alpha), \tag{A8}$$

$$\tilde{S}_v^\alpha = s_v^\alpha + \tfrac{1}{2}\left(s_0 + \frac{s_A^\beta - s_B^\alpha}{2}\right),$$

$$\tilde{S}_v^\beta = s_v^\beta + \tfrac{1}{2}\left(s_0 - \frac{s_A^\beta - s_B^\alpha}{2}\right),$$

$$\tilde{S}_B^\alpha = \tilde{S}_A^\beta = \tfrac{1}{2}(s_A^\beta + s_B^\alpha). \tag{A9}$$

(3) Triple defect systems.

In this case the effective formation energy of a vacancy on one sublattice and an antistructure atom on the other sublattice is lowest, and two vacancies together with one antistructure atom have to be generated simultaneously in order to conserve the homogeneity of the sample. We represent the equations which hold if the vacancy on the α sublattice has the lowest effective formation energy, analogous equations hold for the vacancy on the β sublattice:

$$\tilde{E}_v^\alpha = \tilde{E}_A^\beta = \tfrac{1}{3}(\varepsilon_0 + 2\varepsilon_v^\alpha + \varepsilon_A^\beta),$$

$$\tilde{E}_v^\beta = \varepsilon_v^\beta + \tfrac{1}{3}(2\varepsilon_0 + \varepsilon_v^\alpha - \varepsilon_A^\beta),$$

$$\tilde{E}_B^\alpha = \varepsilon_B^\alpha - \tfrac{1}{3}(\varepsilon_0 + 2\varepsilon_v^\alpha - 2\varepsilon_A^\beta), \tag{A10}$$

$$\tilde{\Omega}_v^\alpha = \tilde{\Omega}_A^\beta = \tfrac{1}{3}(\Omega_0 + 2\Delta V_v^\alpha + \Delta V_A^\beta),$$

$$\tilde{\Omega}_v^\beta = \Delta V_v^\beta + \tfrac{1}{3}(2\Omega_0 + \Delta V_v^\alpha - \Delta V_A^\beta),$$

$$\tilde{\Omega}_B^\alpha = \Delta V_B^\alpha - \tfrac{1}{3}(\Omega_0 + 2\Delta V_v^\alpha - 2\Delta V_A^\beta), \tag{A11}$$

$$\tilde{S}_v^\alpha = \tfrac{1}{3}(s_0 + 2s_v^\alpha + s_A^\beta + k_B \ln 2),$$

$$\tilde{S}_v^\beta = s_v^\beta + \tfrac{1}{3}(2s_0 + s_v^\alpha - s_A^\beta - k_B \ln 2),$$

$$\tilde{S}_A^\beta = \tfrac{1}{3}(s_0 + 2s_v^\alpha + s_A^\beta - 2k_B \ln 2),$$

$$\tilde{S}_B^\alpha = s_B^\alpha - \tfrac{1}{3}(s_0 + 2s_v^\alpha - 2s_A^\beta - 2k_B \ln 2). \tag{A12}$$

2. The nonstoichiometric case

In the nonstoichiometric case analytical expressions may be obtained if the concentration of thermal defects is much smaller than the concentration of the structural defect, and if the type of structural defect is known. Again we illustrate the calculational prescription for one case and then collect the results for all conceivable cases. We thereby represent only the equations for $x > 0.5$. Analogous equations hold for $x < 0.5$ with A, α replaced by B, β and x replaced by $(1-x)$.

(1) The structural defects are A antistructure atoms on the β sublattice. Neglecting the concentrations of the thermal defects, $c_v^\alpha = c_v^\beta = c_B^\alpha = 0$, Eqs. (4) and (3) reduce to

$$c_A^\beta = x - \tfrac{1}{2} \tag{A13}$$

and

$$\varepsilon_0 + p\Omega_0 - Ts_0 = \mu_A + \mu_B - k_B T \ln(1 - 2c_A^\beta). \tag{A14}$$

From Eqs. (A13) and (A14) we calculate the chemical potentials μ_A and μ_B, thereby inserting into Eq. (A13) Eq. (2) and neglecting the exponential in the denominator of Eq. (2) which corresponds to the thermal defect. Inserting these chemical potentials into Eqs. (1) and (2) and neglecting again exponentials corresponding to the thermal defects in the denominators, the concentrations c_i^ν may be written in the form of Eq. (5) with the following effective defect formation quantities:

$$\tilde{E}_v^\alpha = \varepsilon_v^\alpha + \tfrac{1}{2}(\varepsilon_0 + \varepsilon_A^\beta),$$

$$\tilde{E}_v^\beta = \varepsilon_v^\beta + \tfrac{1}{2}(\varepsilon_0 - \varepsilon_A^\beta),$$

$$\tilde{E}_A^\beta = 0,$$

$$\tilde{E}_B^\alpha = \varepsilon_B^\alpha + \varepsilon_A^\beta, \tag{A15}$$

$$\tilde{\Omega}_v^\alpha = \Delta V_v^\alpha + \tfrac{1}{2}(\Omega_0 + \Delta V_A^\beta),$$

$$\tilde{\Omega}_v^\beta = \Delta V_v^\beta + \tfrac{1}{2}(\Omega_0 - \Delta V_A^\beta),$$

$$\tilde{\Omega}_A^\beta = 0,$$

$$\tilde{\Omega}_B^\alpha = \Delta V_B^\alpha + \Delta V_A^\beta, \tag{A16}$$

$$\tilde{S}_v^\alpha = s_v^\alpha + \tfrac{1}{2}(s_0 + s_A^\beta) - \tfrac{1}{2}k_B \ln(2x-1),$$

$$\tilde{S}_v^\beta = s_v^\beta + \tfrac{1}{2}(s_0 - s_A^\beta) + \tfrac{1}{2}k_B \ln(2x-1),$$

$$\tilde{S}_A^\beta = k_B \ln(2x-1),$$

$$\tilde{S}_B^\alpha = s_B^\alpha + s_A^\beta - k_B \ln \frac{2x-1}{2(1-x)}. \tag{A17}$$

It becomes obvious from these equations that in addition to the structural A antistructure atoms on the β sublattice which appear already at zero temperature further A antistructure atoms may be thermally excited in combination with vacancies on the α sublattice or B antistructure atoms on the α sublattice, with activation energies according to $\tilde{E}_v^\alpha$ or $\tilde{E}_B^\alpha$, respectively. Alternatively, A antistructure atoms may be annihilated during the thermal excitation of two vacancies on the β sublattice, if $\tilde{E}_v^\beta$ is smaller than $\tilde{E}_v^\alpha$ and $\tilde{E}_B^\alpha$.

(2) The structural defects are vacancies on the β sublattice

$$\tilde{E}_v^{\alpha}=\varepsilon_v^{\alpha}+\varepsilon_0+\varepsilon_v^{\beta},$$

$$\tilde{E}_v^{\beta}=0,$$

$$\tilde{E}_A^{\beta}=\varepsilon_A^{\beta}-\varepsilon_0-2\varepsilon_v^{\beta},$$

$$\tilde{E}_B^{\alpha}=\varepsilon_B^{\alpha}+\varepsilon_0+2\varepsilon_v^{\beta}, \tag{A18}$$

$$\tilde{\Omega}_v^{\alpha}=\Delta V_v^{\alpha}+\Omega_0+\Delta V_A^{\beta},$$

$$\tilde{\Omega}_v^{\beta}=0,$$

$$\tilde{\Omega}_A^{\beta}=\Delta V_A^{\beta}-\Omega_0-2\Delta V_v^{\beta},$$

$$\tilde{\Omega}_B^{\alpha}=\Delta V_B^{\alpha}+\Omega_0+2\Delta V_v^{\beta}, \tag{A19}$$

$$\tilde{S}_v^{\alpha}=s_v^{\alpha}+s_0+s_A^{\beta}-k_B\ln\frac{2x-1}{x},$$

$$\tilde{S}_v^{\beta}=k_B\ln\frac{2x-1}{x},$$

$$\tilde{S}_A^{\beta}=s_A^{\beta}-s_0-2s_v^{\beta}+2k_B\ln\frac{2x-1}{x},$$

$$\tilde{S}_B^{\alpha}=s_B^{\alpha}+s_0+2s_v^{\beta}-k_B\ln\frac{(2x-1)^2}{x(1-x)}. \tag{A20}$$

Please note that in addition to the structural vacancies on the β sublattice further β vacancies may be generated simultaneously with the excitation of α vacancies or simultaneously with the formation of B antistructure atoms on the α sublattice, with effective formation energies $\tilde{E}_v^{\alpha}$ or $\tilde{E}_B^{\alpha}$, respectively. Alternatively, β vacancies may be annihilated during the thermal excitation of an A antistructure atom on the β sublattice, if $\tilde{E}_A^{\beta}$ is smaller than $\tilde{E}_v^{\alpha}$ and $\tilde{E}_B^{\alpha}$.

In these nonstoichiometric cases the effective formation entropies contain terms which depend only on the composition, which therefore appear even if we neglect the vibrational entropies at all and which may yield negative effective formation entropies. This must be taken into account to avoid misinterpretations of experimental results.[21–23,25,39]

APPENDIX B

In this appendix we show how well converged results (with respect to E_{pw}) for the effective formation energies and volumes may be obtained from not yet converged supercell calculations. The proof is given for a binary compound AB with $B2$ structure, but other structures can be handled accordingly.

The basic idea is that — starting from a reasonably large plane-wave cutoff E_{pw} — the results for the eigenfunctions of a crystal are improved by an increase of E_{pw} mainly in the regions close to the nuclei (where the pseudo wave functions show a strong spatial variation), whereas the results in the binding area between the atoms are only slightly affected. As a result, the deviation of the not yet converged supercell energy from the converged energy is expected to be proportional to the number of nuclei in the supercell. This is also manifested in the fact that the equilibrium lattice constant converges much faster with respect to E_{pw} than the cohesive energy: The energy vs volume curves are more or less rigidly shifted up or down the energy axis when varying E_{pw}. If $E_0(N,c)$ $[E_0(N,nc)]$ denote the energy of the converged (not yet converged) ideal supercell with N atoms, $E_v^{\alpha}(N-1,c)$ $[E_v^{\alpha}(N-1,nc)]$ are the corresponding energies for the supercell with one vacancy on the α sublattice, $E_A^{\beta}(N,c)$ $[E_A^{\beta}(N,nc)]$ are the energies for the supercell with one A antistructure atom on the β sublattice, and if δE_A and δE_B denote the errors per A or B atom due to the nonconverged calculations, we then obtain

$$E_0(N,c)=E_0(N,nc)+\frac{N}{2}\delta E_A+\frac{N}{2}\delta E_B, \tag{B1}$$

$$E_v^{\alpha}(N-1,c)=E_v^{\alpha}(N-1,nc)+\left(\frac{N}{2}-1\right)\delta E_A+\frac{N}{2}\delta E_B, \tag{B2}$$

$$E_A^{\beta}(N,c)=E(N,nc)+\left(\frac{N}{2}+1\right)\delta E_A+\left(\frac{N}{2}-1\right)\delta E_B. \tag{B3}$$

From these equations we obtain

$$\varepsilon_v^{\alpha}(c)=E_v^{\alpha}(N-1,c)-E_0(N,c)=\varepsilon_v^{\alpha}(nc)-\delta E_A, \tag{B4}$$

$$\varepsilon_A^{\beta}(c)=E_A^{\beta}(N,c)-E_0(N,c)=\varepsilon_A^{\beta}(nc)+\delta E_A-\delta E_B. \tag{B5}$$

It becomes obvious that the deviations of the nonconverged defect energy parameters from the converged ones are of the order of $\delta E_A,\delta E_B$, whereas for the energies of the supercells themselves they are of the order of $N\delta E_A,N\delta E_B$.

The same arguments may be applied to the vacancy formation in a monoatomic crystal:

$$E_0(N,c)=E_0(N,nc)+N\delta E, \tag{B6}$$

$$E_v(N-1,c)=E_v(N-1,nc)+(N-1)\delta E. \tag{B7}$$

When calculating the vacancy formation energy

$$\varepsilon_v(c)=E_v(N-1,c)-\frac{N-1}{N}E_0(N,c)$$

$$=E_v(N-1,nc)-\frac{N-1}{N}E_0(N,nc), \tag{B8}$$

the errors per atom δE totally drop out. The supercell calculations for the vacancy formation energy in monoatomic crystals all relied on this error cancellation (see, for instance, Ref. 43). It will be shown in the following that a similar near total error cancellation may be achieved also for the effective formation energies of compounds when in Eq. (3) the nonconverged rather than the converged result for the energy ε_0 per ideal unit cell is inserted. To demonstrate this, we consider Eqs. (1)–(4) and assume that we insert the converged values for $\varepsilon_i^{\nu},\varepsilon_0$, yielding converged values for μ_A and μ_B. Representing these values by

TABLE V. Convergence of the effective Ni vacancy formation energy (in eV) in $B2$-NiAl with respect to E_{pw} (in Ry). The first line (nonconv.) is obtained when using the nonconverged value of ε_0, the second line (conv.) for the use of the converged value. The calculations were performed for an unrelaxed 16-atom supercell and $n_k=56$.

E_{pw}	12.5	16.0	20.0	24.0	30.0	40.0
Nonconv.	0.996	0.992	0.990	0.988	0.988	0.988
Conv.	0.906	0.928	0.945	0.956	0.963	0.986

$$\varepsilon_i^{\nu}(c)=\varepsilon_i^{\nu}(nc)+f(\delta E_A,\delta E_B), \tag{B9}$$

where f denotes the correction terms as given, for instance, in Eqs. (B4) and (B5),

$$\varepsilon_0(c)=\varepsilon_0(nc)+\delta E_A+\delta E_B, \tag{B10}$$

and

$$\mu_{A/B}=\tilde{\mu}_{A/B}+\delta E_{A/B}, \tag{B11}$$

where $\tilde{\mu}_A$ and $\tilde{\mu}_B$ are defined via the last equation, it becomes obvious that all the correction terms δE_A and δE_B drop out in Eqs. (1)–(4). This means that nearly converged results for the concentrations c_i^{ν} may be obtained when inserting in Eqs. (1)–(4) the nonconverged values for ε_i^{ν} *and* ε_0.

To demonstrate the effect, Table V shows the results for the effective vacancy formation energy $\tilde{E}_v^{\alpha}$ for a 16-atom supercell of $B2$-NiAl as obtained by inserting nonconverged or converged values of ε_0, and indeed $\tilde{E}_v^{\alpha}$ converges much faster with E_{pw} when using the nonconverged value of ε_0.

The basic idea has also an implication for the determination of the defect volume parameters ΔV_i^{ν} which are the differences between the equilibrium volumes of the supercell with and without the defect. There are two problems involved in such a calculation. If we calculate the energy of the supercell as function of the volume in order to determine the equilibrium volume, and if we fix the plane-wave cutoff E_{pw}, then the number of plane waves in the basis set which fulfill the cutoff criterion $\hbar^2/2m|\mathbf{k}+\mathbf{G}|^2\leqslant E_{\mathrm{pw}}$ may be different for different volumes because the lengths of the $\mathbf{k}$ vector and the reciprocal-lattice vector $\mathbf{G}$ depend on the volume. Thereby, because of the discrete nature of the reciprocal space the number of plane waves changes discontinously, resulting in discontinuities of the energy vs volume relation. This effect vanishes for $E_{\mathrm{pw}}\rightarrow\infty$ or for the case of infinitely many k points, but it makes the calculation of the equilibrium volumes tedious for small numbers of k points and small E_{pw}. To circumvent the problem,[44] $E_v^{\alpha}(N-1,c)$ is calculated via Eq. (B4), i.e.,

$$E_v^{\alpha}(N-1,c)=E_v^{\alpha}(N-1,nc)-E_0(N,nc)+E_0(N,c)-\delta E_A. \tag{B12}$$

The converged energy $E_0(N,c)$ for the perfect supercell thereby is obtained via

$$E_0(N,c)=\frac{N}{2}E_0(2,c)=\frac{N}{2}\varepsilon_0(c), \tag{B13}$$

where the converged energy $\varepsilon_0(c)$ of the ideal elementary unit cell may be obtained without any problem. Comparing Eqs. (B12) with (B2) demonstrates that when using Eq. (B12) the error of the nonconverged calculation is of the order of magnitude δE_A, whereas it is of the order of $(N/2)\,\delta E_A,(N/2)\,\delta E_B$ when using Eq. (B2). By this numerical trick it is achieved that a smooth energy vs volume curve is obtained for reasonable values of E_{pw}. Because according to our basic idea the energy vs volume curve is shifted more or less rigidly along the energy axis when varying E_{pw} (for reasonably large E_{pw}), the equilibrium volume obtained from the smooth curve for finite E_{pw} nearly coincides with the converged equilibrium volume.

[1] G. Sauthoff, in *Diffusion in Ordered Alloys and Intermetallic Compounds*, edited by B. Fultz, R. W. Cahn, and D. Gupta (TMS, Warrendale, 1993), p. 205.

[2] G. Vaerst, W. Löser, M. Leonhardt, and I. Bächer, Intermetallics **3**, 303 (1995).

[3] H. L. Fraser, M. H. Loretto, R. E. Smallman, and R. J. Wasilewski, Philos. Mag. **28**, 639 (1973).

[4] J. E. Eibner, H.-J. Engell, H. Schultz, H. Jacobi, and G. Schlatte, Philos. Mag. **31**, 739 (1975).

[5] R. Rocktäschl, diploma thesis, University of Stuttgart, 1996.

[6] S. M. Kim, Y. Takeda, and M. Kogachi, Scr. Mater. **34**, 1845 (1996).

[7] V. I. Levit, I. A. Bul, J. Hu, and M. J. Kaufman, Scr. Mater. **34**, 1925 (1996).

[8] S. Frank, C. Herzig, and U. Södervall (private communication).

[9] G. F. Hancock and B. R. McDonnell, Phys. Status Solidi A **4**, 143 (1971).

[10] F. Zobel, Ph.D. thesis, Technical University of Berlin, 1994.

[11] K. Frenner, diploma thesis, University of Stuttgart, 1998; H.-E. Schaefer, K. Frenner, and R. Würschum, Intermetallics (to be published).

[12] U. Essmann, R. Henes, U. Holzwarth, F. Klopfer, and E. Büchler, Phys. Status Solidi A **160**, 487 (1997).

[13] M. Hirscher, D. Schaible, and H. Kronmüller, Phys. Status Solidi A **160**, 507 (1997).

[14] M. S. Daw and M. I. Baskes, Phys. Rev. Lett. **50**, 1285 (1983).

[15] M. Hagen and M. W. Finnis, Philos. Mag. A **77**, 447 (1998).

[16] Y. Mishin and D. Farkas, Defect Diffus. Forum **143-147**, 303 (1997).

[17] W. Kohn and L. J. Sham, Phys. Rev. **140**, A1133 (1965).

[18] C. L. Fu, Y. Y. Ye, M. H. Yoo, and K.-M. Ho, Phys. Rev. B **48**, 6712 (1993).

[19] S. G. Louie, K. M. Ho, and M. L. Cohen, Phys. Rev. B **19**, 1774 (1979); C. Elsässer, N. Takeuchi, K. M. Ho, C. T. Chan, P. Braun, and M. Fähnle, J. Phys.: Condens. Matter **2**, 4371 (1990).

[20] B. Meyer, C. Elsässer, and M. Fähnle, FORTRAN 90 program for mixed-basis pseudopotential calculations for crystals, Max-Planck Institut für Metallforschung, Stuttgard (unpublished).

[21] J. Mayer and M. Fähnle, Acta Mater. **45**, 2207 (1997).
[22] M. Fähnle, J. Mayer, and B. Meyer, Intermetallics (to be published).
[23] J. Mayer, C. Elsässer, and M. Fähnle, Phys. Status Solidi B **191**, 283 (1995).
[24] J. Mayer and M. Fähnle, Scr. Mater. **37**, 131 (1997).
[25] M. Fähnle, G. Bester, and B. Meyer, Scr. Mater. **39**, 1071 (1998).
[26] G. Bester, B. Meyer, and M. Fähnle, Phys. Rev. B **57**, 11 019 (1998).
[27] W. Frank, U. Breier, C. Elsässer, and M. Fähnle, Phys. Rev. Lett. **77**, 518 (1996).
[28] J. P. Perdew and A. Zunger, Phys. Rev. B **23**, 5048 (1981).
[29] D. Vanderbilt, Phys. Rev. B **32**, 8412 (1985).
[30] S. G. Louie, S. Froyen, and M. L. Cohen, Phys. Rev. B **26**, 1738 (1982).
[31] D. J. Chadi and M. L. Cohen, Phys. Rev. B **8**, 5747 (1973).
[32] C.-L. Fu and K. M. Ho, Phys. Rev. B **28**, 5480 (1983).
[33] C. Elsässer, M. Fähnle, C. T. Chan, and K. M. Ho, Phys. Rev. B **49**, 13 975 (1994).
[34] M. J. Cooper, Philos. Mag. **8**, 805 (1963).
[35] N. Rusović and H. Warlimont, Phys. Status Solidi A **44**, 609 (1977).
[36] R. Krachler, H. Ipser, and K. L. Komarek, Z. Metallkd. **73**, 731 (1982).
[37] R. Krachler, H. Ipser, and K. L. Komarek, J. Phys. Chem. Solids **50**, 1127 (1989).
[38] V. Schott and M. Fähnle, Phys. Status Solidi B **204**, 617 (1997).
[39] M. Fähnle, B. Meyer, J. Mayer, J. S. Oehrens, and G. Bester, in *Diffusion Mechanisms in Crystalline Materials*, edited by Y. Mishin *et al.*, MRS Symposia Proceedings No. 527 (Materials Research Society, Pittsburgh, 1998), p. 23.
[40] K. Badura-Gergen, Ph.D. thesis, University of Stuttgart, 1995.
[41] O. G. Randl, G. Vogl, M. Kaisermayr, W. Bührer, J. Pannetier, and W. Petry, J. Phys.: Condens. Matter **8**, 7689 (1996).
[42] A. J. Bradley and A. Taylor, Proc. R. Soc. London, Ser. A **159**, 56 (1937).
[43] R. Pawellek, M. Fähnle, C. Elsässer, K. M. Ho, and C. T. Chan, J. Phys.: Condens. Matter **3**, 2451 (1991).
[44] U. Breier, W. Frank, C. Elsässer, M. Fähnle, and A. Seeger, Phys. Rev. B **50**, 5928 (1994).